

# NONCOLOCATION EFFECTS ON THE RIGID BODY ROTORDYNAMICS OF ROTORS ON AMB

Giancarlo Genta

Department of Mechanics, Politecnico di Torino, Torino, Italy, genta@polito.it

Stefano Carabelli

Department of Automatic Control, Politecnico di Torino, Torino, Italy, carabelli@polito.it

## ABSTRACT

The effect of sensor-actuator non-collocation on the behaviour of machines running on active magnetic bearings is studied under the assumptions that the rotor behaves as a rigid body, the controller is an ideal decentralized proportional-derivative one, the behaviour of the bearings can be linearized and the whole machine is axially symmetrical. The possible presence of an instability range, which in some cases can extend down to the zero-speed condition, is demonstrated. The effect of damping on the instability range is studied, showing that it is stabilizing and that, with damping high enough, it is possible to achieve stable running in the whole working range. A simple centralized controller which cures the consequences of non-collocation is shown to exist and its gains are computed. The paper includes also an example related to an actual machine showing strong non-collocation effects.

## INTRODUCTION

Noncollocation between sensors and actuators is a well known problem for flexible structures [2, 3]. With magnetic bearing technology, it must be taken into account in the design stage, as it can introduce non-negligible effects in the dynamic behaviour of the machine, and even lead to instabilities.

There is no difficulty in doing so when modelling the system using the finite element method; however it is usually not considered when simpler models, as the well known four-degrees-of-freedom (two if working using complex coordinates), model are used. Such a simple approach is well suited for the very common case of machines working well below the flexural critical speeds of the rotor and through the rigid-body critical speeds, which in the case of AMB may have a fairly low value. In such a speed range the rotor can be considered as a rigid body.

If the feedback loop is modeled with an ideal PD controller, the very simple nature of the model allows to perform a general rotordynamic study, yielding interesting results. In particular it is possible to study the effect of the non-collocation and to show that it introduces a type of behaviour which can be quite different from that typical of rotors running on conventional bearings. An instability range can be present, and in some extreme cases the system may

even be unstable at standstill.

The instability range can be shown to shrink with increasing damping (i.e. the derivative gain of the control loop).

As the analysis deals only with the rigid-body dynamics, it doesn't allow to predict possible spillover effects, in which higher modes may be excited by the control system, particularly owing to non-collocation effects. However, if the maximum operating speed is well below the first critical speed linked with the deformation of the rotor and the controller doesn't introduce a large phase loss in the vicinity of the higher natural frequencies of the system, the internal damping of the rotor can successfully deal with spillover problems and the present analysis is well applicable, at least in producing a reduced order model for the design of the electromechanical parts and the control system.

## ANALYSIS

### Equations of motion

Consider a rigid rotor running on  $n$  active magnetic bearings (AMB). Assume that  $z$  axis of the inertial reference frame  $Gxyz$  centered in the position of the center of mass of the rotor at rest  $G$  coincides with the rotation axis and let  $z_i$  and  $z'_i$  be the  $z$ -coordinates of the sensor and the actuator of the  $i$ -th bearing.

The lateral behaviour can be modeled using the following equation of motion written in complex coordinates

$$\mathbf{M}\ddot{\mathbf{q}} - i\omega\mathbf{G}\dot{\mathbf{q}} = \mathbf{F}_c + \mathbf{F}_n + \omega^2\mathbf{F}_r, \quad (1)$$

where

$$\mathbf{M} = \begin{bmatrix} m & 0 \\ 0 & J_t \end{bmatrix}, \quad \mathbf{G} = \begin{bmatrix} 0 & 0 \\ 0 & J_p \end{bmatrix}, \quad \mathbf{q} = \begin{Bmatrix} x + iy \\ \phi_y - i\phi_x \end{Bmatrix}$$

and  $\mathbf{F}_c$ ,  $\mathbf{F}_n$  and  $\mathbf{F}_r$  are the control forces, the nonrotating forces and the rotating forces due to unbalance (see [1]).

Assume that the controller is an ideal decentralized PD controller and that the law expressing force  $\mathbf{F}_i$  (in complex notation) exerted by the  $i$ -th actuator as a function of the displacements  $x_i + iy_i$  and  $x'_i + iy'_i$  at the  $i$ -th sensor and actuator locations and the velocity at the  $i$ -th sensor is:

$$+\alpha - \beta^2 + \gamma^2 = 0.$$

$$\mathbf{F}_i = -K_i(x_i + iy_i) - K_i C_i(\dot{x}_i + i\dot{y}_i) + K_{u_i}(x'_i + iy'_i). \quad (2)$$

where and  $K_i$  and  $C_i$  are the gains of the control loop, while  $K_{u_i}$  is them open-loop destabilizing stiffness of the bearing.

By introducing the control force vector  $\mathbf{F}_c$  due to a number  $n$  of actuators into Eq. (1) and defyning the average distance of the  $i$ -th sensor-actuator pair  $\bar{z}_i = \frac{1}{2}(z_i + z'_i)$  and the noncolocation  $z_{i_d} = \frac{1}{2}(z_i - z'_i)$  of the same pair, the equation of motion of the system reduces to

$$\mathbf{M}\ddot{\mathbf{q}} + (\mathbf{C} - i\omega\mathbf{G})\dot{\mathbf{q}} + \mathbf{K}\mathbf{q} = \mathbf{F}_n + \omega^2\mathbf{F}_r, \quad (3)$$

where

$$\mathbf{K} = \begin{bmatrix} k_1 & k_2 \\ k_2 & k_3 \end{bmatrix} + \begin{bmatrix} 0 & -k_4 \\ k_4 & 0 \end{bmatrix},$$

$$k_1 = \sum_{i=1}^n (K_i - K_{u_i}), \quad k_4 = \sum_{i=1}^n K_i z_{i_d},$$

$$k_2 = \sum_{i=1}^n (K_i \bar{z}_i - K_{u_i} z'_i),$$

$$k_3 = \sum_{i=1}^n (K_i [\bar{z}_i^2 - z_{i_d}^2] - K_{u_i} z_i'^2),$$

$$\mathbf{C} = \begin{bmatrix} c_1 & c_2 \\ c_2 & c_3 \end{bmatrix} + \begin{bmatrix} 0 & -c_4 \\ c_4 & 0 \end{bmatrix},$$

$$c_1 = \sum_{i=1}^n C_i K_i, \quad c_2 = \sum_{i=1}^n C_i K_i \bar{z}_i,$$

$$c_3 = \sum_{i=1}^n C_i K_i (\bar{z}_i^2 - z_{i_d}^2), \quad c_4 = \sum_{i=1}^n C_i K_i z_{i_d}.$$

Owing to noncolocation ( $z_i \neq z'_i$ ), matrices  $\mathbf{C}$  and  $\mathbf{K}$  are non symmetrical and may be non-positive defined. The presence of the negative terms due to  $K_{u_i}$  is usually not causing problems in colocated systems, owing to their smallness, but in the present case they may contribute to make the stiffness matrix non-positive defined.

The skew-symmetric part of matrix  $\mathbf{K}$  is usually referred to as a circulatory matrix; it contains only noncolocation effects due to distances  $z_{i_d}$ .

### Study of the stability

Consider the homogeneous equation associated with Eq. (1). Assuming a solution of the type  $\mathbf{q} = \mathbf{q}_0 e^{i\lambda t}$ , where vector  $\mathbf{q}$  contains the complex coordinates  $x + iy$  and  $\phi_y - i\phi_x$ , and solving the related eigenproblem, the following nondimensional characteristic equation allowing to compute the whirling frequencies is obtained

$$\begin{aligned} & \lambda'^4 - [\omega'\delta + 2i(\zeta + \eta\alpha)]\lambda'^3 + \quad (4) \\ & - [1 + \alpha + 2\zeta\eta\alpha - 2\theta\kappa(\beta^2 - \gamma^2) - 2i\omega\zeta\delta]\lambda'^2 + \\ & + [\omega'\delta + 2i\alpha(\zeta + \eta) - 2i(\beta^2 - \gamma^2)(\theta + \kappa)]\lambda' + \end{aligned}$$

where the nondimensional complex whirl frequency  $\lambda' = \lambda/\lambda_1$  and the nondimensional spin speed  $\omega' = \omega/\lambda_1$  have been defined with reference to the natural frequency  $\lambda_1 = \sqrt{k_1/m}$  of a Jeffcott rotor with the same mass and a stiffness equal to  $k_1$ .

Eq. (4) depends only on eight nondimensional parameters, namely

-‘elastic’ parameters:

$$\alpha = \alpha' + \alpha''$$

$$\alpha' = \frac{m}{J_t} \frac{\sum_{i=1}^n (K_i \bar{z}_i^2 - K_{u_i} z_i'^2)}{\sum_{i=1}^n (K_i - K_{u_i})}$$

$$\alpha'' = -\frac{m}{J_t} \frac{\sum_{i=1}^n K_i z_{i_d}^2}{\sum_{i=1}^n (K_i - K_{u_i})}$$

$$\beta = \frac{\sum_{i=1}^n (K_i \bar{z}_i - K_{u_i} z'_i)}{\sum_{i=1}^n (K_i - K_{u_i})} \sqrt{\frac{m}{J_t}},$$

$$\gamma = \frac{\sum_{i=1}^n K_i z_{i_d}}{\sum_{i=1}^n (K_i - K_{u_i})} \sqrt{\frac{m}{J_t}},$$

-‘inertial’ parameter:  $\delta = J_p/J_t$ ,

-‘damping’ parameters:

$$\zeta = \frac{C_{11}}{2K_{11}}\lambda_1, \quad \eta = \frac{C_{22}}{2K_{22}}\lambda_1, \quad \theta = \frac{C_{12}}{2K_{12}}\lambda_1, \quad \kappa = \frac{C_{21}}{2K_{21}}\lambda_1.$$

Note that:

- $\alpha$  is made of two parts, namely  $\alpha'$  and  $\alpha''$ . The first one does not depend on the non-colocation but only on the average positions  $\bar{z}_i$  and is always positive;  $\alpha''$  vanishes for colocated systems and is always negative.
- $\beta$  does not depend on the non-colocation as  $\alpha'$ , can be either positive or negative and vanishes for symmetrical systems (see below).
- $\gamma$  can be positive or negative and vanishes for either colocated or symmetrical systems.
- The sign of  $\beta$  and  $\gamma$  has no effect on the behaviour of the system, as only the squares of these parameters are included in the equations.
- $\delta$  is the usual parameter for gyroscopic effects; its value can span from 0 (long rotors) to 2 (disc rotors); however a smaller variability range is expected in actual applications.
- $\zeta$  coincides with the damping ratio of the above mentioned Jeffcott rotor. If all the bearings have the same derivative gain  $C_i$  and the contributions due to the terms  $K_{u_i}$  are small enough to be neglected,  $\eta = \theta = \kappa = \zeta$  and the number of relevant nondimensional parameters reduces to five.

As the equation has complex coefficients, the solutions are complex but not conjugate. Although little can be said in general on the stability of the system, Eq. (4) allows to assess numerically the stability in any given case.

In the case of the undamped system, Eq. (4) reduces to

$$\lambda'^4 - \omega'\delta\lambda'^3 - (1 + \alpha)\lambda'^2 + \omega\delta\lambda' + \alpha - \beta^2 + \gamma^2 = 0, \quad (5)$$

which depends on just four nondimensional parameters.

The latter equation has real coefficients: the solutions can be real numbers, in which case the system is stable (in the sense that the amplitude of free whirling neither decreases nor increases in time), or complex conjugate numbers. In the latter case, at least one solution with negative imaginary part exists and the system is unstable.

### Symmetrical system

Consider a rotor on two equal bearings with its center of mass at midspan. Assume that also the sensors are symmetrically located. The equations of motion for the translational and rotational degrees of freedom uncouple (only four nondimensional parameters are different from zero, namely  $\alpha$ ,  $\delta$ ,  $\zeta$  and  $\eta$ ) and the characteristic Eq. (4) splits into two independent equations:

$$\begin{cases} -\lambda'^2 + 2i\zeta\lambda' + 1 = 0 \\ -\lambda'^2 + \omega'\delta\lambda' + 2i\eta\alpha\lambda' + \alpha = 0 \end{cases} \quad (6)$$

Cylindrical whirling is governed by the same equation of the well known equation of motion of the Jeffcott rotor. The equation describing the conical whirling differs from the usual equation dealing with co-located systems because the product  $z_1 z_1'$  can be negative in the case the actuator on one side is connected with the sensor on the other one. In this case  $\alpha$  is negative.

If  $\alpha$  is positive, the behaviour of the system is equal to that of a co-located system with the actuator in the position  $z_1^* = \sqrt{z_1 z_1'}$ . The case with negative  $\alpha$  has very little practical interest, as the system is unstable at standstill, behaving as a spring, mass, damper system with negative stiffness and damping coefficient. However the gyroscopic moment can stabilize the undamped system.

The solution of the second Eq. (6) is

$$\lambda' = \frac{\omega'\delta + 2i\eta\alpha \pm \sqrt{(\omega'\delta + 2i\eta\alpha)^2 + 4\alpha}}{2} \quad (7)$$

which holds for both  $\alpha$  positive or negative.

If  $\alpha$  is negative, it follows:

$$\Re(\lambda') = \frac{\omega'\delta}{2} \pm \sqrt{\frac{\sqrt{a^2 + b^2} + a}{2}}, \quad (8)$$

$$\Im(\lambda') = -\eta|\alpha| \mp \sqrt{\frac{\sqrt{a^2 + b^2} - a}{2}}, \quad (9)$$

where  $a = \omega'^2\delta^2 - 4\delta^2\alpha^2 - 4|\alpha|$  and  $b = 4\omega'\delta\eta|\alpha|$ .

In the case of the undamped system, stability occurs if

$$\omega > \frac{2\sqrt{|\alpha|}}{\delta}. \quad (10)$$

However, the presence of damping make the system unstable at all speeds since the imaginary part of one of two values of  $\lambda'$  is always negative for any value of the spin speed  $\omega'$ .

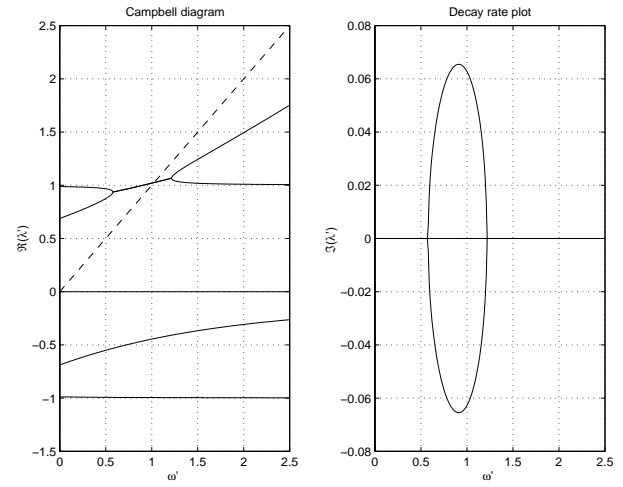


**FIGURE 1:** Nondimensional campbell diagram the decay rate plot of a system with  $\alpha' = 0.5$ ,  $\alpha'' = 0.05$ ,  $\beta = 0.1$ ,  $\gamma = 0.15$  and  $\delta = 0.6$ .

### Non-symmetrical system

If the center of mass of the rotor is not at midspan or if the symmetry assumed in the previous section is violated, the two equations of motion do not uncouple and the modes do not reduce to conical and cylindrical ones. Nevertheless often they are still referred to as conical or cylindrical, but only in a general way, as the first one does not have its vertex in the center of mass and the latter is not a true cylinder.

The condition for stability of the undamped system at standstill is

$$(1 - \alpha)^2 + 4\beta^2 - 4\gamma^2 > 0, \quad (11)$$

which is obviously verified for  $\beta > \gamma$ , although being less restrictive than that.

The equations become complicated enough to prevent from performing a closed form general study of the stability, even in the undamped case. Although little can be said in general on the stability of the system, Eq. (4) allows to assess numerically the stability in any given case.

Some typical plots and conclusions drawn from numerical experimentation on undamped systems will be reported here. The nondimensional campbell diagram and the decay rate plot of a system with  $\alpha' = 0.5$ ,  $\alpha'' = 0.05$ ,  $\beta = 0.1$ ,  $\gamma = 0.15$  and  $\delta = 0.6$  are reported in Fig. 1. The system is stable for  $\omega = 0$ , as  $(1 - \alpha)^2 + 4\beta^2 - 4\gamma^2 = 0.2525 > 0$ .

The curves related to cylindrical and conical whirling cross in the first quadrant and, where they meet, a field of instability starts. The unstable conditions persist up to a certain speed, which is beyond the crossing of the Campbell diagram with the line  $\lambda' = \omega'$ .

The plot is repeated in Fig. 2, with the same values of the parameters, but with  $\delta = 1.5$  instead of  $\delta = 0.6$ , i.e., with a disc rotor instead of a long rotor.

The results are similar to the one previously seen, with the difference that the curve related to the conical mode in forward whirling (whose asymptote is

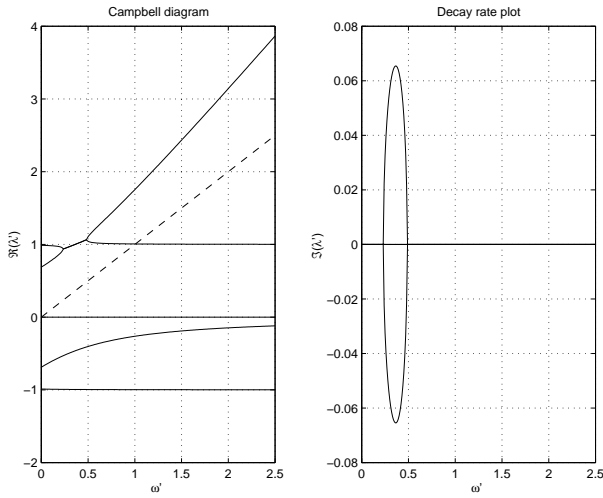


**FIGURE 2:** Nondimensional campbell diagram the decay rate plot of a system with  $\alpha' = 0.5$ ,  $\alpha'' = 0.05$ ,  $\beta = 0.1$ ,  $\gamma = 0.15$  and  $\delta = 1.5$ .

the straight line with equation  $\lambda' = \omega' J_p / J_t$ ) has a greater slope. As a result the instability range moves toward lower speeds and lies all in the subcritical range (on the left of the line  $\lambda' = \omega'$ ).

The plot of Fig. 3 deals with the same values of the parameters as in Fig. 1 (long rotor), but for the values of  $\alpha'$  which is now greater than 1 (2 instead of 0.5). The curves related to cylindrical and conical whirling now cross in the fourth quadrant and, consequently, the field of instability occurs in backward whirling conditions.

The plot of Fig. 4 refers to the same case of Fig. 3, but for a disc rotor ( $\delta = 1.5$  instead of  $\delta = 0.6$ ). As  $\alpha' > 1$  the instability range lies in the backward whirl zone of the plot, but it is displaced towards lower values of the speed.

Note that in all cases studied above an instability range was present. Further numerical investigation showed that this is due to the fact that  $\gamma > \beta$ . If, on the contrary  $\gamma < \beta$ , no instability range was encountered, at least unless  $\alpha'' > \alpha'$ . The conclusions drawn from the numerical experiments run on undamped system are reported in the following table

	crossing in	$\gamma < \beta$	$\gamma > \beta$
$\alpha' < 1$	I quadrant	no inst.	unst. FWD modes
$\alpha' > 1$	IV quadrant	no inst.	unst. BWD modes

A further case, with the same parameters of that studied in Fig. 1, but with  $\alpha' = 1.1$ , is shown in Fig. 5. Note that now  $(1 - \alpha)^2 + 4\beta^2 - 4\gamma^2 = -0.0475 < 0$ : the system is unstable even at standstill, for both forward and backward modes, to be stabilized at high speed by the gyroscopic effect.

The effect of damping is that of reducing the width of the instability range and, if the system is damped enough, no instability is encountered.

## GEOMETRIC RE-COLOCATION

Consider a rotor running on two magnetic bearings. If the rotor is rigid, the noncolocation effect can be

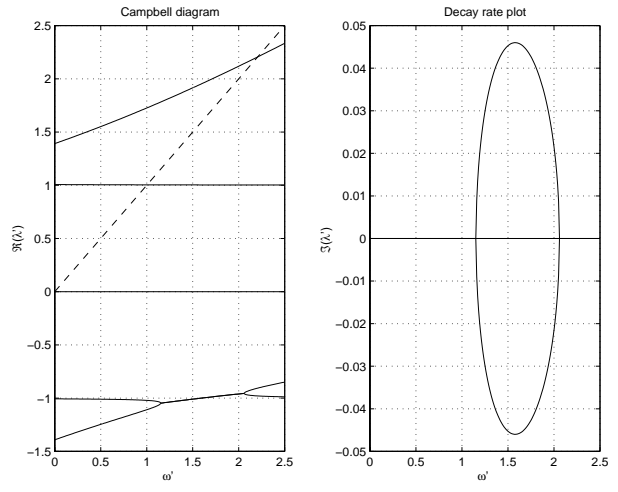


**FIGURE 3:** Nondimensional campbell diagram the decay rate plot of a system with  $\alpha' = 2$ ,  $\alpha'' = 0.05$ ,  $\beta = 0.1$ ,  $\gamma = 0.15$  and  $\delta = 0.6$ .

compensated for by using a centralized control system, i.e. it is possible to design a centralized control system which causes the actuators to produce forces which are proportional to the displacements (or the velocity, for the derivative branch of the control loop), at the actuator locations instead of that of the sensors.

The complex displacements at the sensor and actuator locations can be expressed as functions of the displacement and rotation at the center of gravity as

$$\begin{Bmatrix} x_1 + iy_1 \\ x_2 + iy_2 \end{Bmatrix} = \mathbf{T} \begin{Bmatrix} x + iy \\ \phi_y - i\phi_x \end{Bmatrix} \quad (12)$$

$$\begin{Bmatrix} x'_1 + iy'_1 \\ x'_2 + iy'_2 \end{Bmatrix} = \mathbf{T}' \begin{Bmatrix} x + iy \\ \phi_y - i\phi_x \end{Bmatrix} \quad (13)$$

where

$$\mathbf{T} = \begin{bmatrix} 1 & z_1 \\ 1 & z_2 \end{bmatrix}, \quad \mathbf{T}' = \begin{bmatrix} 1 & z'_1 \\ 1 & z'_2 \end{bmatrix}$$

The proportional part of the forces exerted by the actuators are proportional to the displacements at the actuator location if

$$\begin{Bmatrix} F_{x_1} + iF_{y_1} \\ F_{x_2} + iF_{y_2} \end{Bmatrix} = \begin{bmatrix} K_1 & 0 \\ 0 & K_2 \end{bmatrix} \mathbf{T}' \mathbf{T}^{-1} \begin{Bmatrix} x_1 + iy_1 \\ x_2 + iy_2 \end{Bmatrix} \quad (14)$$

The matrix of the gains of the control system required perform the relocation is thus

$$\begin{aligned} \mathbf{K}_c &= \begin{bmatrix} K_1 & 0 \\ 0 & K_2 \end{bmatrix} \mathbf{T}' \mathbf{T}^{-1} = \\ &= \frac{1}{z_1 - z_2} \begin{bmatrix} K_1(z'_1 - z_2) & K_1(z_1 - z'_1) \\ K_2(z'_2 - z_2) & K_2(z_1 - z'_2) \end{bmatrix} \end{aligned} \quad (15)$$

The matrix of the derivative gains can be obtained in the same way, just substituting  $C_i K_i$  for  $K_i$ .

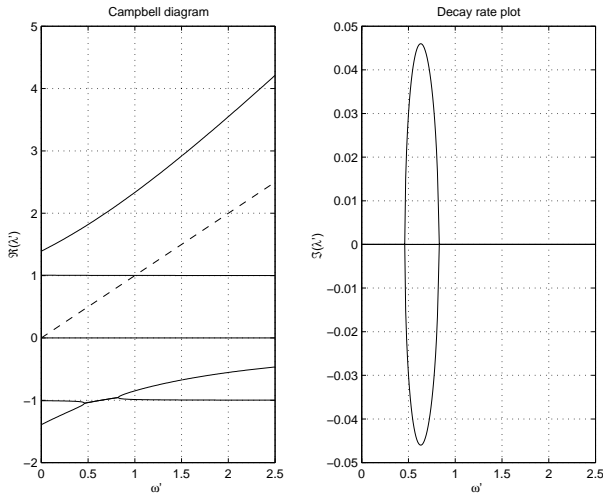


**FIGURE 4:** Nondimensional campbell diagram the decay rate plot of a system with  $\alpha' = 2$ ,  $\alpha'' = 0.05$ ,  $\beta = 0.1$ ,  $\gamma = 0.15$  and  $\delta = 1.5$ .

### EXAMPLE

Consider a rotor with the following inertial data:  $m = 9.270$  kg;  $J_t = 0.0800$  kg m<sup>2</sup>;  $J_p = 0.0337$  kg m<sup>2</sup>. The center of mass of the rotor is at 134.5 mm from one end of the shaft while the actuators and sensors are at 128.7 mm, 250.8 (actuators), 90.1 mm and 219.5 mm (sensors) respectively. The gains of the sensor-actuator loop of the bearings are  $K_1 = 2.2 \times 10^6$  N/m and  $K_2 = 0.6 \times 10^6$  N/m,  $K_{u_1} = 32,000$  N/m and  $K_{u_2} = 36,000$  N/m.

The nondimensional parameters of the undamped system are:  $\alpha = 0.2620$  ( $\alpha' = 0.3030$ ,  $\alpha'' = 0.0410$ ),  $\beta = 0.0199$ ,  $\gamma = 0.2043$  and  $\delta = 0.4212$ . The value of  $\lambda_1$  is  $\lambda_1 = 542.8$  rad/s.

The system is stable for  $\omega = 0$ , as  $(1 - \alpha)^2 + 4\beta^2 - 4\gamma^2 = 0.378 > 0$ . The campbell diagram of the undamped system is shown in Fig. 6.

As expected the branches of the Campbell diagram meet in the first quadrant ( $\alpha' < 1$ ), a field of instability exists ( $\gamma > \beta$ ) and is located mainly in the supercritical field ( $\delta < 1$ ).

The computation of the Campbell diagram was repeated with different non-colocations and values of the damping to obtain stability maps with the aim of assessing stability boundaries. The results are reported in Fig. 7 in which the spin speeds at which the rotor becomes unstable and then stable again are plotted as functions of the distance  $d$  between the sensors and the actuators.

The various curves have been obtained for different values of the damping ratio  $\zeta$ . Note that the sensor-actuator distance has been assumed to be the same for the two bearings (which is not the case in the actual system) and also the controllers have been assumed to supply the same derivative action (equal  $C_i$ ). Strictly speaking, the values of  $\zeta$ ,  $\eta$ ,  $\theta$  and  $\kappa$  are not exactly equal.

If the sensor-actuator distance is smaller than 20 mm no instability occurs even if the system is undamped, while larger sensor-actuator distances lead to increasingly large instability ranges.

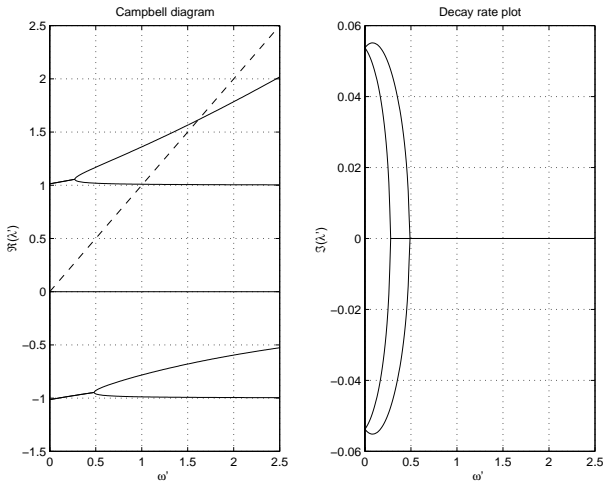


**FIGURE 5:** Nondimensional campbell diagram the decay rate plot of a system with  $\alpha' = 1.1$ ,  $\alpha'' = 0.05$ ,  $\beta = 0.1$ ,  $\gamma = 0.15$  and  $\delta = 0.6$ . As  $(1 - \alpha)^2 + 4\beta^2 - 4\gamma^2 = -0.0475 < 0$  the system is unstable for  $\omega' = 0$ .

By adding damping the maximum value of  $d$  for which the system is stable increases and, if the unstable range is at any rate found, the threshold of instability increases with the damping. The value of the upper limit of the instability range has a more complex behaviour: the presence of damping causes it to increase, but then it decreases with further increases of damping.

As the average sensor-actuator distance is of 35 mm, a damping ratio in excess of 0.175 is required to guarantee stability. A larger value of damping, i.e.  $C_1 = C_2 = 1 \times 10^{-3}$  is assumed, to account for the fact that the larger bearing which has a larger non-colocation (due to a greater bulk of the actuator). It leads to a stable system with  $\zeta = 0.278$ ,  $\eta = 0.286$ ,  $\theta = 0.262$  and  $\kappa = 0.279$ .

The matrix of the gains of a centralized control system able to relocate the system, is

$$\begin{bmatrix} 2.896 & -0.696 \\ 0.154 & 0.446 \end{bmatrix} \times 10^6 \text{ N/m}$$

The Campbell diagram of the undamped system is reported in Fig. 8: its overall pattern is that of a conventional rotor on soft bearings and no non-colocation effect is present

### CONCLUSIONS

The sensor-actuator non-colocation may have a detrimental effect on the behaviour of machines running on active magnetic bearings. Some bearing configurations, mainly those based on optical sensors, allow positioning the sensors and the actuators in the same location, thus avoiding the problem from its onset, but in the majority of cases non-colocation is the rule.

The distance between sensors and actuators depends on the actual layout of the machine, and in some cases cannot be reduced owing to the length of the pole pieces of the actuators and, in a number

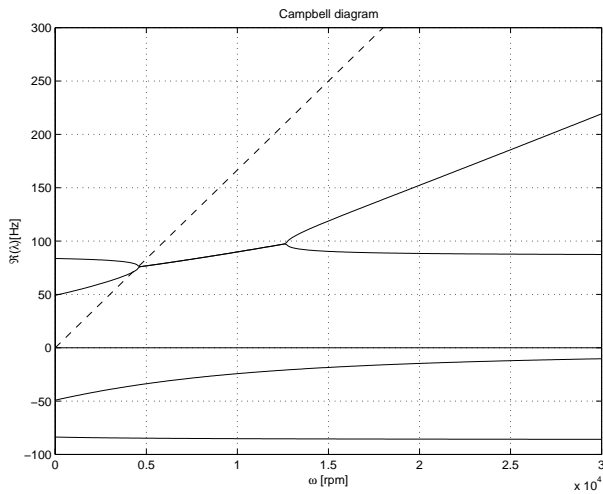


**FIGURE 6:** Campbell diagram of the system studied in the example (undamped system).

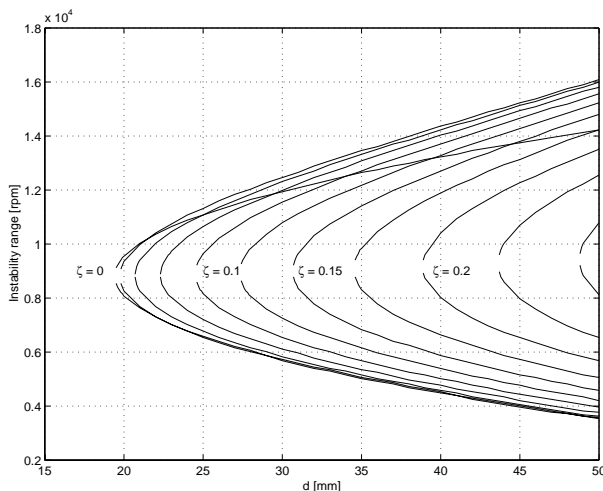


**FIGURE 7:** Lower and upper limits of the instability range as functions of the sensor-actuator distance, for various values of the damping ratio  $\zeta$ .

of cases, the need of avoiding interferences on the sensors.

As long as the rotor may be assumed as rigid, the sensor-actuator noncolocation is commonly thought not to be a problem, in any case a problem to be considered only for machines designed to work well above the rigid body critical speeds where flexible modes come into play.

The effect of noncolocation has been studied here under the assumptions that the rotor behaves as a rigid body, the controller is an ideal decentralized proportional-derivative one, the behaviour of the bearings can be linearized and the whole machine is axially symmetrical. Under these conditions the effect of the non-colocation is to introduce a skew-symmetric part into both the closed-loop stiffness and damping matrices and even to make the overall matrices non-positive defined. The outcome is the possible presence of an instability range, which

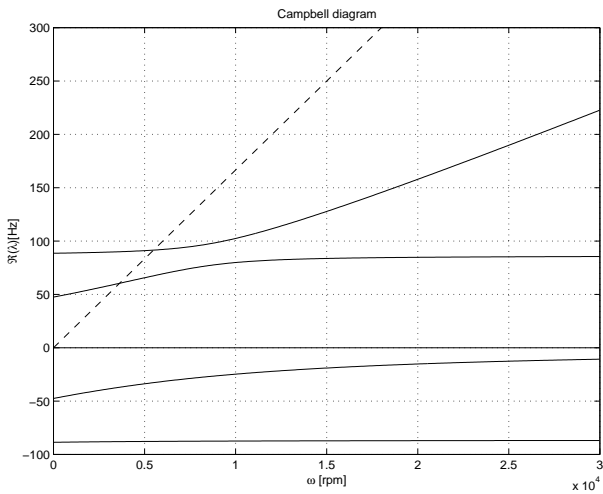


**FIGURE 8:** Campbell diagram of the same system of Fig. 7, but with a centralized controller which re-locates sensors and actuators (undamped system).

in some cases may extend down to zero-speed.

With some combinations of the values of the parameters the mode which can become unstable is a forward whirling mode, in other cases a backward mode is unstabilized.

The presence of damping reduces the width of the instability range and, if the damping is high enough, stable running can be achieved in the whole working range.

As only the rigid-body behaviour has been considered, it is possible to use a centralized controller to cure the consequences of non-colocation, obtaining the dynamic behaviour typical of collocated systems. This procedure has been here referred to as geometric re-colocation.

The results here obtained are linked with the rigid-body assumptions and hold only in the speed range extending to speeds well below the first critical speed linked with rotor deformations. Many machines running on magnetic bearings however operate in these conditions, so they are applicable to many actual cases.

An example related to a turbomolecular pump, on which the effects of noncolocation were first observed, shows how the analytical results apply to an actual machine.

## REFERENCES

- [1] G. Genta, *Vibration of Structures and Machines*, 3rd ed., Springer, New York, 1998.
- [2] R. Cannon and D. Rosenthal, *Experiments in control of flexible structures with noncollocated sensors and actuators*, AIAA Journal of Guidance, vol. 7, pp. 546–553, Sept.-Oct. 1984.
- [3] V. Spector and H. Flashner, *Modeling and design implications of noncollocated control in flexible systems*, ASME Journal of Dynamic Systems, Measurement, and Control, vol. 112, pp. 186–193, June 1990.